BNL-61540

CYLINDRICAL SHELL BUCKLING THROUGH STRAIN HARDENING[1]

K. Bandyopadhyay, J. Xu and S. Shteyngart
Brookhaven National Laboratory
Upton, New York

D. Gupta
U.S. Department of Energy
Germantown, Maryland

ABSTRACT

Recently, the authors published results of plastic buckling analysis of cylindrical shells. Ideal elastic-plastic material behavior was used for the analysis. Subsequently, the buckling analysis program was continued with the realistic stress-strain relationship of a stainless steel alloy which does not exhibit a clear yield point. The plastic buckling analysis was carried out through the initial stages of strain hardening for various internal pressure values. The computer program BOSOR5 was used for this purpose. The results were compared with those obtained from the idealized elastic-plastic relationship using the offset stress level at 0.2% strain as the yield stress. For moderate hoop stress values, the realistic stress-strain case shows a slight reduction of the buckling strength. But, a substantial gain in the buckling strength is observed as the hoop stress approaches the yield strength. Most importantly, the shell retains a residual strength to carry a small amount of axial compressive load even when the hoop stress has exceeded the offset yield strength.

INTRODUCTION

The axial compressive strength of a perfect cylinder can be obtained by using the classical elastic shell theory. In reality, due to the presence of unavoidable geometric imperfections, the strength is far less than this classical solution. Internal pressure, if present, can reduce the geometric imperfections and the shell regains some of the lost compressive strength. At high internal pressure when the hoop stress is a large fraction of the material yield strength, the biaxial stress state plays a key role in controlling the shell compressive strength, and plastic collapse is predicted prior to elastic bifurcation buckling. These shell behaviors have been extensively studied in the literature [NASA, 1968; ECCS, 1988; Miller, 1991; Bandyopadhyay, 1993; Priestley, 1986; Rotter, 1985 and 1989; Saal, 1977; Vandepitte, 1980]. Recently, the authors summarized these results and compared with their own analytical work [Bandyopadhyay, 1994]. Elastic-perfectly-plastic stress-strain curves were used in these shell buckling and plastic collapse analyses. In order to determine the effects of a realistic stress-strain relationship on the compressive strength, further analyses have been performed. This paper presents the results of these analyses.

SHELL GEOMETRY

The geometry considered in the analysis is the same used in earlier studies [Bandyopadhyay, 1993 and 1994]. A 40-foot high circular cylinder contains an inward bulge of shape (1-cosθ) located at the bottom (Figure 1). The length of the bulge, L, is given in terms of the radius, R, and shell thickness, t, as follows:

$$L = 4.0\sqrt{Rt} \qquad (1)$$

The magnitude of the bulge in the radial direction, e, is given by

[1] The study was sponsored by the U.S. Department of Energy, Office of Environmental Restoration and Waste Management (DOE-EM).

$$e = 0.01L \qquad (2)$$

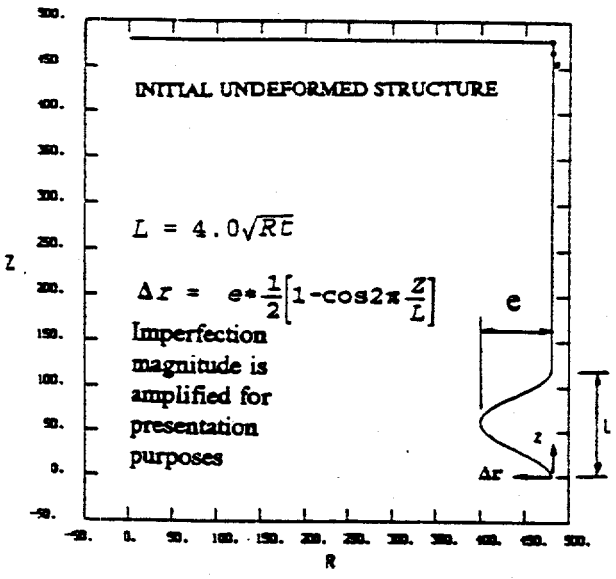

Figure 1 Modeled Imperfection Shape

STRESS-STRAIN CURVES

The cylinder is assumed to be fabricated from a stainless steel alloy (304). The corresponding stress-strain curves are shown in Figure 2. Curve A shows the actual (still there is some approximation in interpolation of test data) stress-strain relationship. As expected, the material does not have a clearly defined yield strength. Considering the offset stress at 0.2% strain as the yield strength, the ideal elastic-plastic relationship is exhibited by Curve B. Near the yield strength, Curve B shows higher strength and stiffness than Curve A. At a higher strain, Curve A shows strain hardening that is obviously absent for the elastic-plastic relationship, i.e., Curve B.

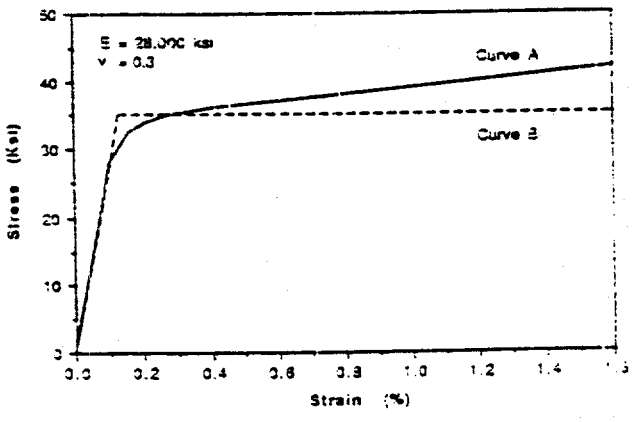

Figure 2 Stress-Strain Curves for 304 Stainless Steel

ANALYSIS RESULTS

The cylinder has been analyzed by using the BOSOR5 computer program [Bushnell, 1974]. First, similar to earlier work [Bandyopadhyay, 1994], the analysis has been performed with the idealized elastic-plastic curve for the geometry considered in this paper. The buckling/collapse stresses at internal pressure, p, and for R/t = 400, 900 and 1500 are presented in Figure 3. The axial stress, σ_{axial}, is nondimensionalized with respect to the classical elastic buckling stress, σ_{cl}. Similarly, the hoop stress is nondimensionalized with the yield strength, F_y. The results are then compared with the ECCS [ECCS, 1988] and New Zealand Code [Priestley, 1986] formulas shown in Figures 4 through 7. The BOSORS results compare well with the Code results. As reported in earlier work, in the plastic range, a better correlation is observed with the New Zealand results, and also with the ECCS results provided the additional factor of safety is reduced to 1.

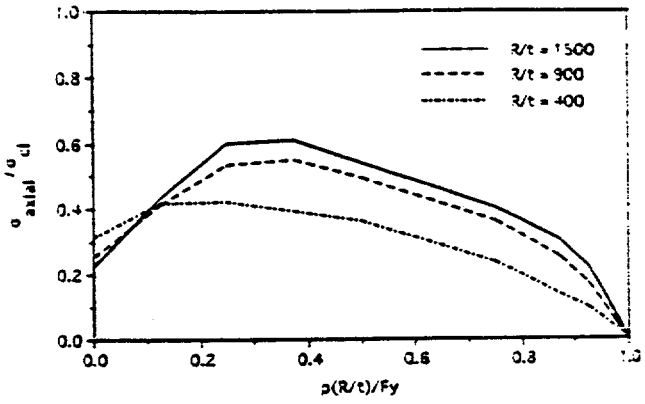

Figure 3 Influence of Internal Pressure on Axial Compressive Strength for Idealized Stress-Strain Relationship (Curve B)

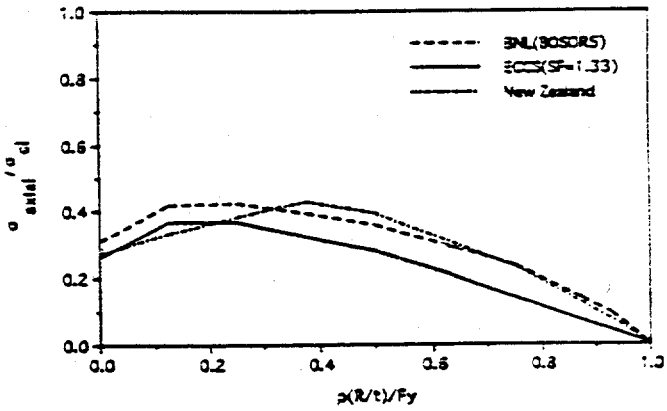

Figure 4 Comparison of Axial Compressive Stresses for R/t = 400 (Curve B)

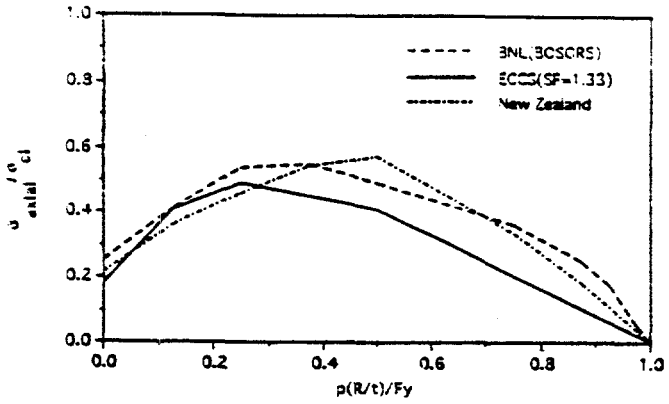

Figure 5 Comparison of Axial Compressive Stresses for R/t = 900 (Curve B)

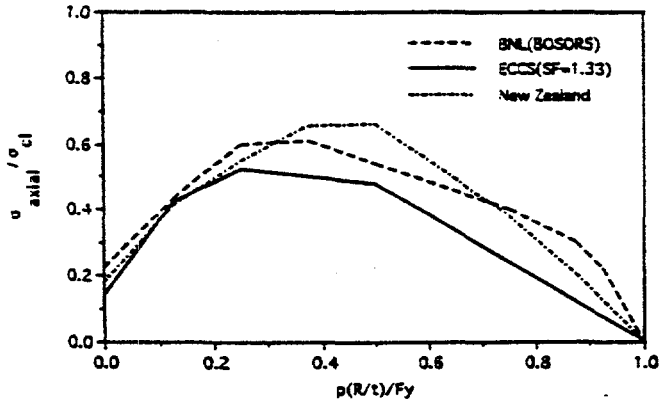

Figure 6 Comparison of Axial Compressive Stresses for R/t = 1500 (Curve B)

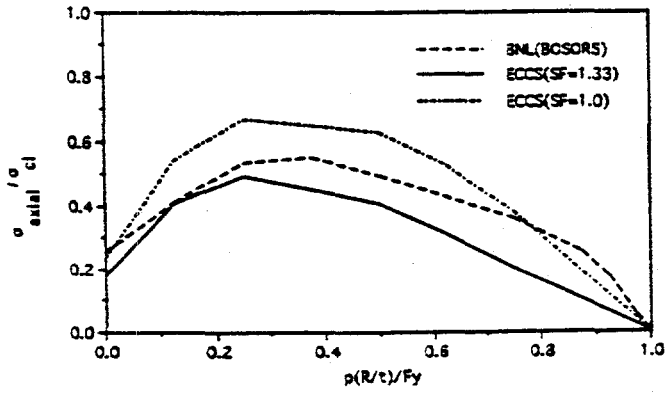

Figure 7 Comparison of Axial Compressive Stresses with ECCS Formulas using SF = 1.00 and 1.33 (Curve B), R/t = 900

Next, the analysis was prepared for R/t = 900 by using the realistic stress-strain relationship (i.e., Curve A), and the results are compared with those already obtained for Curve B (Figure 8). Very little difference between the two sets of results is observed at low internal pressure. As pressure increases, a slight reduction of the axial strength is noted for Curve A due to the unconservative values of the stress and stiffness for Curve B near the idealized yield point as mentioned earlier. However, a significant difference between the two curves is observed at high pressures when hoop stresses approach and exceed the yield strength. This is due to the strain hardening effect available with the real stress-strain diagram, i.e., Curve A. Most importantly, the shell retains a residual compression-carrying capacity at and even beyond the point where the hoop stress reaches the material yield strength. This residual compressive strength is the result of the stiffness that remains only with the real stress-strain curve (i.e., Curve A) rather than the idealized elastic-plastic curve (i.e., Curve B).

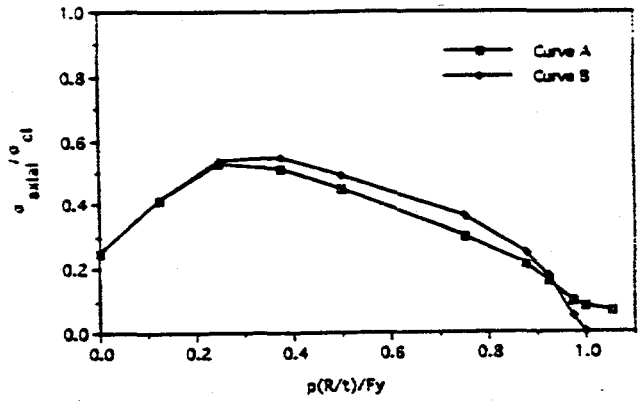

Figure 8 Strain-Hardening Effect on Buckling of Cylindrical Shell, R/t = 900

The corresponding displacements of the cylindrical shell as the axial load increases for a given hoop stress are shown in Figures 9 through 12. Both axial and radial displacements are plotted. The initial axial deformation corresponds to the effect of the hoop stress (i.e., Poisson's effect). As the axial load increases, the deformation for Curve A compared to that for Curve B becomes larger.

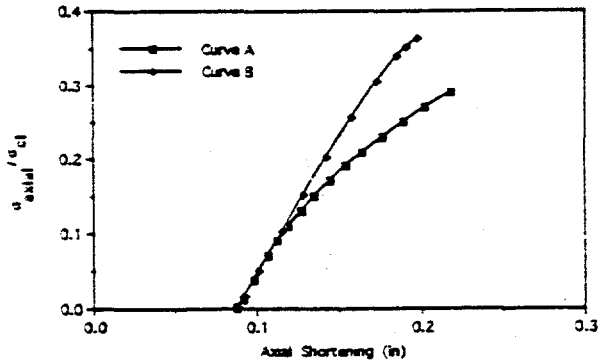

Figure 9 Load-Deflection Curves: Axial Shortening σ_{hoop}/F_y = 0.75, R/t = 900

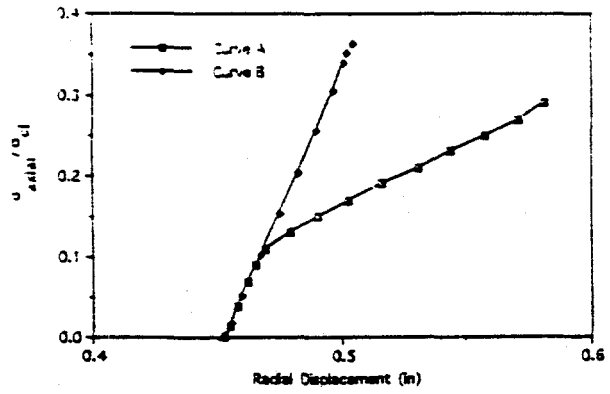

Figure 10 Load-Deflection Curves: Radial Displacement
σ_{hoop}/F_y = 0.75, R/t = 900

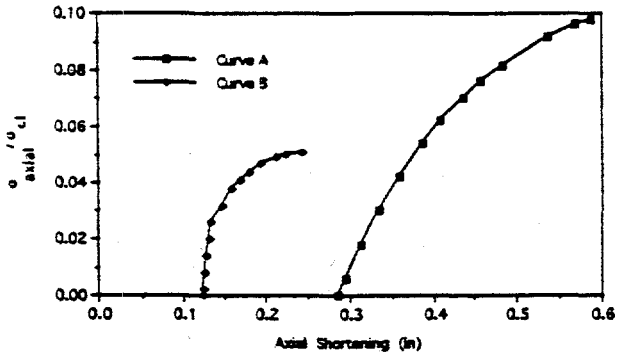

Figure 11 Load-Deflection Curves: Axial Shortening
σ_{hoop}/F_y = 0.975, R/t = 900

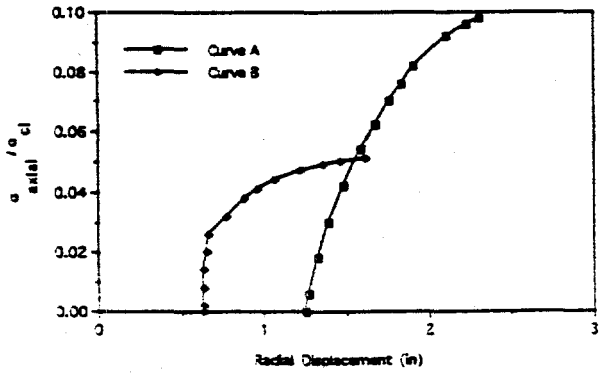

Figure 12 Load-Deflection Curves: Radial Displacement
σ_{hoop}/F_y = 0.975, R/t = 900

DISCLAIMER

Another major difference between the results of the two stress-strain curves is in the failure mode. For the elastic-perfectly-plastic curve, at low pressure the shell buckles first and at high pressure plastic collapse governs the axial strength. For the realistic stress-strain curve, the controlling failure mode is buckling since some amount of stiffness remains even at a high strain. For example, in Figure 8 (Curve A), when the hoop stress reaches the yield strength (i.e., offset stress at 0.2% strain), the effective plastic strain is 0.53% indicating steady stiffness at that point (Figure 2, Curve A).

SUMMARY AND CONCLUSIONS

If a real stress-strain curve is used instead of an idealized perfectly elastic-plastic curve, the following observations can be made:

- At small internal pressure, there is no difference between the buckling capacities corresponding to the two sets of data.

- At moderate internal pressure (e.g., hoop stress = 0.25 to 0.9 of yield strength), there is small reduction of the axial compressive strength for the real stress-strain curve.

- For large internal pressure with the hoop stress approaching the yield strength, the buckling capacity reduces gradually for the real stress-strain curve compared to the sharp decline for the perfectly elastic-plastic relationship.

- For a hoop stress at or slightly beyond the yield strength, a residual axial compressive strength is observed for the real stress-strain curve.

- The failure mode for the ideal elastic-plastic curve is buckling at low pressure and plastic collapse at high pressure. The failure mode for the real stress-strain relationship is buckling until the hoop stress exceeds the yield strength; beyond this, the large strain may control the design depending on how large a strain can be accepted.

Unlike a finite element model, the BOSOR5 mathematical model does not become adjusted for large strain and produces some amount of computational error. Therefore, although the above observations seem to be consistent with earthquake experience data that indicate residual axial strength even when the hoop stress reaches the material yield strength, the exact values need to be verified with an appropriate independent finite element analysis model. The authors expect to present such results in a future publication.

ACKNOWLEDGEMENTS

The authors are grateful to the DOE Program Director, Mr. John Tseng, for his encouragement and support. The authors sincerely acknowledge the advice, cooperation and comments of Drs. David Bushnell, Robert Kennedy, Anestis Veletsos, Charles Miller, Carl Costantino and Allin Cornell.

REFERENCES

Bandyopadhyay, K., Xu, J., Shteyngart, S., and Eckert, H., "Plastic Buckling of Cylindrical Shells," PVP-Vol. 271, Natural Hazard Phenomena and Mitigation, ASME, pp. 33-37, 1994.

Bandyopadhyay, K., Xu, J., and Shteyngart, S., "Buckling Analysis of Cylindrical Waste Tank Shell," 4th DOE NPH Mitigation Conference, Atlanta, GA, October, 1993.

"Buckling of Thin-Walled Circular Cylinders," NASA SP-8007, National Aeronautics and Space Administration, August 1968.

Bushnell, D., "BOSOR5: A Computer Program for Buckling of Elastic-Plastic Complex Shells of Revolution including Large Deflection and Creep," Lockheed Missiles & Space Co., December 1974.

ECCS, "Buckling of Steel Shells - European Recommendations," Fourth Edition, 1988.

Miller, C.D., "ASME Code Case N-284, Metal Containment Shell Buckling Design Methods," May 1991.

Priestley, M.J.N., et al., "Seismic Design of Storage Tanks - Recommendations of a Study Group of the New Zealand National Society for Earthquake Engineering," December 1986.

Rotter, J.M., "Buckling of Ground-Supported Cylindrical Steel Bins Under Vertical Compressive Wall Loads," Metal Structures Conferences, Melbourne, Australia, May 23-25, 1985.

Rotter, J.M., and J.G. Teng, "Elastic Stability of Cylindrical Shells with Weld Depressions," ASCE, Journal of Structural Engineering, Vol. 115, No. 5, May 1989.

Saal, H., "Buckling of Circular Cylindrical Shells under Combined Axial Compression and Internal Pressure," ECCS Second International Colloquium, Stability of Steel Structures, Liege 13-15, April 1977.

Vandepitte, D. and J. Rathe, "Buckling of Circular Cylindrical Shells under Axial Load in the Elastic-Plastic Region," Der Stahlbau, Heft 12, 1980.

DISCLAIMER